PHYSICAL REVIEW A VOLUME 27, NUMBER 3 MARCH 1983

First- and second-order transitions to superstructures: Relation to discrete maps

E. Allroth and H. Müller-Krumbhaar
Institut für Festkörperforschung der Kernforschungsanlage, Jülich, Postfach 1913, 5170 Jülich, West Germany
(Received 23 September 1982)

A variational model for an incommensurate epitaxial layer on a relaxing substrate is studied. The corresponding two-dimensional area-preserving maps allow no conclusion about the existence of a phase transition. Explicit expressions for the free energy show the occurrence of second- or first-order transitions, depending upon parameters. The resulting phase diagram is related to a "complete devil's staircase."

I. INTRODUCTION

In this paper we investigate the old problem of superstructures with incommensurability or long periods relative to a lattice unit in the light of the recent progress in discrete dynamical systems. Pioneering work in this direction was performed by Aubry[1] and we use his approach as a guideline for the present analysis.

We restrict ourselves to a model in one space dimension, which describes either an infinite one-dimensional atomic chain coupled to a lattice, or a higher-dimensional system with mean field averaging over all dimensions except one, a standard approximation in the theory of crystal growth.

The basic Frenkel-Kontorova[2] model for epitaxy and its dynamical analog, the Chirikov model,[3] have attracted great attention in recent years, since the resulting recursion relations are one of the simplest examples of two-dimensional area-preserving maps showing complicated incommensurate Kolmogorov-Arnold-Moser (KAM) and chaotic trajectories.

For the understanding of a discrete dynamical system it is—by definition—quite sufficient to study the properties of the corresponding map in detail. For the present evaluation of minimum (free-) energy configurations of discrete atomistic chains, however, it is not sufficient to perform the variation on the (free-) energy functional and then merely study the resulting recursion equations. These equations do not discriminate between the state of absolutely minimal energy and local minima over even maxima. This is particularly obvious for systems exhibiting first-order phase transitions as a function of parameters. Here the typically two competing states of the system are each in a local energy minimum, and only the comparison between the absolute energies—a nonlocal property—discriminates the actual "ground" state. This means also that the study of phonon stability is not sufficient to find the ground state since it merely ensures the state to be in a local minimum.

Unfortunately, the infinite summations involved in an evaluation of the (free) energy generally cannot be performed analytically in a nonlinear system. To make the situation worse, the use of a computer is also of only little help. Even for the simple case of a two-dimensional map—corresponding to nearest-neighbor interaction in a chain—one would have to scan a two-dimensional continuum. Clearly one cannot detect incommensurate trajectories and because of rounding errors one will not be able to discriminate between hyperbolic fixed points of high order and neighboring chaotic trajectories.

At present, therefore, one is restricted to either approximations such as the continuum approximation[2(b),4,5] to the discrete system or to simplifications such as a substitution of the nonlinear model by a piecewise linear model. This latter simplification, of course, may miss some important features, such as KAM trajectories, but allows us to maintain the discrete character of the original model.

In Sec. II we will introduce the model. In Sec. III we derive explicit formulas for the free energy. In Sec. IV the exact results are used to discuss the nature of the phase transition together with the concept of the devil's staircase. The procedure of Sec. III is, as far as possible, generalized in Sec. V. Section VI gives concluding remarks.

II. EPITAXIAL MODEL WITH SUBSTRATE RELAXATION

We investigate a model for an epitaxial layer on a substrate with lattice mismatch between the adsorbed layer and the substrate. It is an extension of the Frenkel-Kontorova (FK) model, since the substrate may undergo

surface reconstruction to partially adjust its (surface-) lattice constant to the adsorbate. It is a discrete version of a continuum model[4] discussed previously. Our extended Frenkel-Kontorova (eFK) model is one dimensional in space, its free energy (in the mean-field sense) is given by

$$F=\frac{1}{N}\left[\sum_n\{\tfrac{1}{2}(\phi_{n+1}-\phi_n-\Delta)^2-\tfrac{1}{2}\Delta^2+\rho[1-\cos(\phi_n)]\}+\sum_{m(n)}[\tfrac{1}{2}c\eta_m^2+\tfrac{1}{2}d(\eta_{m+1}-\eta_m)^2]\right.$$
$$\left.+\sum_{n,m(n)}W_{mn}\eta_m(\phi_n-\phi_{n-1})\right], \tag{1}$$

where $N\to\infty$ and Δ denotes the lattice mismatch of the uncoupled adsorbate and substrate. The phase difference of the adsorbate atom n relative to the (unperturbed) substrate potential is denoted by ϕ_n. Denoting the displacement of the mth atom of the surface row of the substrate by S_m, we assume harmonic interaction energy $\sim(\eta_m)^2$, where $\eta_m=S_{m+1}-S_m$ is the local strain. In principle, one now has to sum over all the bulk atoms in the substrate to produce an effective long-range elastic interaction. We model this here in a crude way by merely including the next term $\sim(\eta_{m+1}-\eta_m)^2$ in the interaction energy. Alternatively, this term also naturally appears due to interactions longer than those between nearest neighbors in a single chain.

We now come to the coupling between adsorbate and substrate. Most naturally, the substrate potential acting on the adsorbate (here $\sim\cos\phi_n$) will be deformed by the relaxing substrate thus reducing the strength of the effective substrate potential. For small substrate response the leading correction is linear in η and ϕ and included here as $\sim\eta_m(\phi_n-\phi_{n-1})$.

A further problem occurs in the counting of ϕ_n and η_m. Because of the lattice mismatch, generally, there is no one-to-one correspondence of adsorbate and substrate atoms. This is formally taken into account by using different indices n and m for the two fields ϕ_n and η_m and an index-dependent coupling constant $W_{m,n}$. Because of the crude approximation for the longer-ranged elastic effects in the substrate, however, we may safely ignore this problem at least for sufficiently small relative lattice mismatch or resulting kink density. We therefore replace m by n and replace the coupling matrix $W_{m,n}$ by an averaged constant value. The strain η_n then corresponds to a slab directly associated with the adsorbate phase ϕ_n. In the most interesting region of long-ranged superstructures this simplification cannot possibly result in qualitative changes of the systems behavior, but can only lead to small quantitative corrections in energies and kink densities.

As a last point we will replace the nonharmonic potential $\cos(\phi_n)$ by a piecewise harmonic array of parabolas in order to allow for explicit evaluations of the free energy. This simplification will result in the nonexistence of KAM trajectories and generally in the absence of incommensurate superstructures. The practical importance of this simplification will be discussed in Sec. III.

It will be useful for comparison with the continuum version of the model to rescale the coupling constants by setting

$$v=\frac{W}{\sqrt{c}} \tag{2}$$

and

$$u=\frac{\rho d}{c}\ . \tag{3}$$

Scaling the strains by

$$\xi_n=\sqrt{c}\,\eta_n \tag{4}$$

we arrive at the final form of our free energy

$$F(u,v,\rho,\Delta)=\frac{1}{N}\sum_n\left[\tfrac{1}{2}(\phi_{n+1}-\phi_n-\Delta)^2-\tfrac{1}{2}\Delta^2+\rho V(\phi_n)+v\xi_n(\phi_n-\phi_{n-1})+\tfrac{1}{2}\xi_n^2+\frac{1}{2}\frac{u}{\rho}(\xi_{n+1}-\xi_n)^2\right], \tag{5}$$

where

$$V(\phi_n)=1-\cos\phi_n \tag{6}$$

will be replaced by a piecewise harmonic potential at a later point in the forthcoming analysis.

III. CLOSED-FORM GROUND-STATE FREE ENERGIES

At a given value of the parameters u,v,ρ,Δ thermal equilibrium requires the system to be in a

state of minimal free energy. This ground state thus requires the following derivatives to vanish for all lattice sites n:

$$\frac{\partial F}{\partial \phi_n}=0\ ,\quad \frac{\partial F}{\partial \xi_n}=0\ , \tag{7}$$

which explicitly gives

$$\begin{aligned} 0&=\phi_{n+1}+\phi_{n-1}-2\phi_n-\rho V'(\phi_n)\\ &\quad +v(\xi_{n+1}-\xi_n)\ ,\\ 0&=\frac{u}{\rho}(\xi_{n+1}+\xi_{n-1}-2\xi_n)-\xi_n-v(\phi_n-\phi_{n-1})\ . \end{aligned} \tag{8}$$

Introducing difference variables $\psi_n=\phi_n-\phi_{n-1}$ and $\chi_n=\xi_n-\xi_{n-1}$, this system of second-order difference equations is transformed into a system of first-order equations

$$\begin{aligned} \psi_{n+1}&=\psi_n+\rho V'(\phi_n)-v\chi_{n+1}\ ,\\ \phi_{n+1}&=\phi_n+\psi_{n+1}\ ,\\ \frac{u}{\rho}\chi_{n+1}&=\frac{u}{\rho}\chi_n+\xi_n+v\psi_n\ ,\\ \xi_{n+1}&=\xi_n+\chi_{n+1}\ . \end{aligned} \tag{9}$$

Equations (9) can be interpreted as a four-dimensional nonlinear volume-preserving map T: Knowing the values of χ,ξ,ψ,ϕ at site n, T gives us those at site $n+1$, etc. We want to point out once more that the map alone cannot give any information about the selection of the ground state or about the kind of possible phase transitions: The first statement is immediately clear since the essential misfit Δ is missing in (9); the second will be demonstrated below.

We will now perform the minimization of F [Eq. (5)] in two steps. We look first for the minimizing configuration of (9) and its free energy F_l at a given winding number l,

$$l=\lim_{N-N'\to\infty}\frac{\phi_N-\phi_{N'}}{N-N'}\frac{1}{2\pi}\ . \tag{10}$$

In the second step we then minimize F_l with respect to l. This point will require some further attention, since F_l is nonanalytic in l. The winding number (10) is the discrete analog of the soliton density playing the role of the order parameter in the continuous case.[4] The terms identical to the FK model then give the contribution F_l^0 to the free energy:

$$F_l^0(\rho,\Delta)=\frac{1}{N}\sum_n \tfrac{1}{2}\psi_n^2+\rho V(\phi_n)-2\pi l\Delta\ . \tag{11}$$

A. Limits of no coupling to the substrate, soft and stiff strain field

At vanishing coupling $v=0$ the map splits into two independent two-dimensional maps: (a) the map $T^{\psi,\phi}(\rho)$ resulting from (11), which is with the potential (6) just the well-investigated[3] Chirikov map and (b) the linear map $T^{\chi,\xi}(\rho/u)$ for the strain variables.

We will now comment upon these maps briefly. $T^{\chi,\xi}$ is, of course, exactly resolvable. It has the fixed point $(\chi_0,\xi_0)=(0,0)$. For all physically acceptable parameter values the fixed point is hyperbolic: the area-preserving map $T^{\chi,\xi}$ then has the real eigenvalues $e^{\pm\gamma_0(\rho/u)}$, where

$$e^{\pm\gamma_0(x)}=1+\frac{x}{2}\pm(x+x^2/4)^{1/2}\ . \tag{12}$$

$\gamma_0(\rho/u)$ is thus just the Lyapunov exponent of $T^{\chi,\xi}$.

The Chirikov map in connection with the FK model, on the other hand, has been extensively analyzed by Aubry.[1] These points follow from his work:

(i) Each ground state is characterized by a well-defined winding number l.

(ii) If $l=r/s$, with r and s irreducible integers, the ground state has periodicity (modulo 2π) s: $\phi_{n+s}=\phi_n+2\pi r$; it is commensurate of order s. In the mapping it is represented by the hyperbolic fixed points of $(T^{\psi,\phi})^s$.

(iii) If l is irrational and the corresponding KAM trajectory exists, it represents the incommensurate ground state of that winding number. The existence of the KAM trajectory implies a zero gap in the excitation spectrum (i.e., a phason mode exists).

(iv) Chaotic mapping states do not appear as ground states.

We return now to the case $v\neq 0$ of nonvanishing coupling between phase and strain field: There are two other limiting cases of the eFK model, which essentially can be reduced to the simpler FK model.

If the medium has negligible stiffness, $d=u=0$, Eq. (9) yields

$$\xi_n=-v\psi_n\ . \tag{13}$$

We then arrive at the renormalized (Chirikov) map $T^{\psi,\phi}(\rho/1-v^2)$

$$\begin{aligned} \psi_{n+1}&=\psi_n+\frac{\rho}{1-v^2}V'(\phi_n)\ ,\\ \phi_{n+1}&=\phi_n+\psi_{n+1}\ . \end{aligned} \tag{14}$$

With (13) the free energy can be described by

$$\begin{aligned} &F_l(u=0,v,\rho,\Delta)\\ &\quad=(1-v^2)F_l^0\left[\frac{\rho}{1-v^2}\ ,\frac{\Delta}{1-v^2}\right]\ . \end{aligned} \tag{15}$$

Thus if we know the ground states of the FK model for arbitrary potential strength ρ and misfit values

Δ, we know them for the eFK model with vanishing stiffness $u=0$ too. The renormalized parameters remain always positive, since stability arguments guarantee

$$v^2<1$$

[see the comments to Eq. (47)].

In the opposite limit of an infinitely stiff substrate $u=\infty$ (which allows only for homogeneous contraction), the mapping (9) requires $\chi_n=\chi_0$. χ_0, however, has to be equal to zero because of energy considerations. Thus only one strain variable

$$\xi_n=\zeta_0 \tag{16}$$

survives. Minimizing

$$F_l(u=\infty,v,\rho,\Delta)=F_l^0(\rho,\Delta)+\tfrac{1}{2}\xi_0^2+v\xi_0 l 2\pi \tag{17}$$

with respect to ζ_0 yields

$$\xi_0=-vl2\pi \tag{18}$$

and

$$F_l(u=\infty,v,\rho,\Delta)=F_l^0(\rho,\Delta)-\tfrac{1}{2}(2\pi vl)^2 . \tag{19}$$

Thus there are two most interesting limiting cases where, despite small formal modifications, the free energy can be reduced to that of the FK model.

B. Closed-form expressions for F_l^0

For an analytic investigation of these cases we will now find expressions for $F_l^0(\rho,\Delta)$ in closed form. This cannot be achieved for the cosine potential (6), but we are able to do it for an array of parabolas

$$V(\phi_n)=\tfrac{1}{2}(\phi_n-2\pi m_n)^2 \tag{20}$$

with

$$m_n=\mathrm{Int}\left[\frac{\phi_n}{2\pi}+\tfrac{1}{2}\right], \tag{21}$$

where $\mathrm{Int}(x)$ means the greatest integer number smaller than or equal to x. The quantity m_n gives just the number of the parabola basin in which the nth particle resides (Fig. 1). Ground-state configurations in this periodic potential have to obey the mapping equations

$$\begin{aligned}\psi_{n+1}&=\psi_n+\rho(\phi_n-2\pi m_n) ,\\ \phi_{n+1}&=\phi_n+\psi_{n+1} .\end{aligned} \tag{22}$$

Equations (22) are only correct if none of the particles sits on a potential cusp. But configurations with a particle on a cusp are excluded from the set

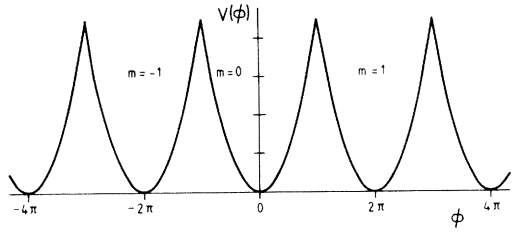

FIG. 1. Periodic potential [Eq. (20)] and basin number m [Eq. (21)].

of ground-state configurations. We show this in the following way. Let us assume the existence of a ground state with at least one particle on top of a potential cusp. This particle feels no force from the periodic potential and therefore the neighboring particles are placed symmetrically around its position. Now we displace only this particle. The nearest-neighbor interaction energy increases quadratically in the displacement variable while the periodic potential decreases linearly for small displacements; i.e., we can gain energy by slightly displacing the particle from the cusp, and hence it is not a minimum-energy configuration.

Contrary to the FK model with a cosine potential the parabola system has no KAM trajectories, however weak the potential may be. Moreover, for the parabola system all fixed points are hyperbolic. Both properties yield map plots looking still more chaotic (Fig. 2) than those (meanwhile well known) for the everywhere analytic cosine potential.[3] These differences, however, are of minor importance for the evaluation of the order parameter l characterizing the phase transition. Using the continued-fraction representation of an irrational number l, this can be approximated as accurately as desired by a rational number; the difference between a really incommensurate (KAM) trajectory and a trajectory which is commensurate of very high order is of academic interest only, concerning the physical consequences.

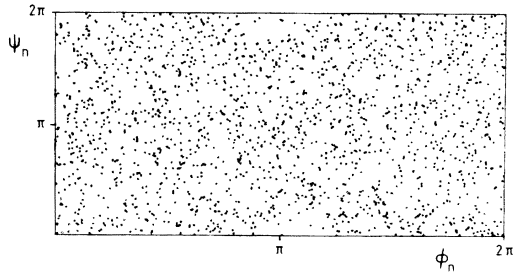

FIG. 2. Trajectories (ϕ_n,ψ_n) of the map [Eq. (22)] for $0\le n\le 200$ and with $\rho=0.2$, $\phi_0=0.0$, and $\psi_0=1.0,1.5,\ldots,5.0$.

With the use of (22) one can express the phases by the basin numbers m_n and arrives at

$$F_l^0(\rho,\Delta) = -2\pi l\Delta + \frac{\pi^2\rho^2}{(\rho+\rho^2/4)^{1/2}} \sum_{n>0} e^{-n\gamma_0(\rho)} \Omega_n^{(2)}(l) \tag{23}$$

with the second moment

$$\Omega_n^{(2)}(l) = \frac{1}{N} \sum_i^{(l)} (m_{i+n} - m_i)^2 . \tag{24}$$

The index l denotes the fixed winding number and thus the fixed first moment

$$\Omega_n^{(1)}(l) = \frac{1}{N} \sum_i (m_{i+n} - m_i) = nl . \tag{25}$$

As we know from Aubry's work[1] any ground state of the FK system is described by

$$m_n = \mathrm{Int}(nl+\alpha) . \tag{26}$$

With (25) and (26) the second moment $\Omega_n^{(2)}(l)$ can be written as

$$\Omega_n^{(2)}(l) = -\mathrm{Int}(nl)^2 - \mathrm{Int}(nl) + nl[1+2\,\mathrm{Int}(nl)] . \tag{27}$$

F_l^0 is therefore reduced[1] to an infinite n sum over an explicitly known function of n. Aubry used this expression to prove that $l(\Delta)$ is a complete devil's staircase for the parabola system. What does this mean? At the boundaries of an interval $I=\{\Delta_i,\Delta_f\}$, $\Delta_i<\Delta_f$, the ground-state winding number l may be given by the rational numbers r_i and $r_f>r_i$, respectively. If, now, between Δ_i and Δ_f *all*—everywhere dense—rational numbers between r_i and r_f appear as ground states with a nonvanishing Δ range each, $l(\Delta)$ is a complete devil's staircase in the interval I. Looking at I with a bad resolution only a finite number of the broadest stairs are seen. Looking at the Δ range between two consecutive stairs with better resolution new stairs become visible, etc.

Instead of evaluating (23) with (27) numerically, we now show how the infinite summation can be done explicitly. So we will be able to give free energies for the piecewise parabolic FK model ($v=0,u\neq 0$) and the cases of soft strain field ($u=0,v\neq 0$) and stiff strain field ($u=\infty,v\neq 0$) of the coupled system. With the definition

$$d_n(l) = nl - \mathrm{Int}(nl) \tag{28}$$

we write the second moment (27) as

$$\Omega_n^{(2)}(l) = (nl)^2 + d_n(l)[1-d_n(l)] . \tag{29}$$

Thus the nontrivial sum to be done remains

$$S(l) = \sum_{n=1}^{\infty} e^{-\gamma_0(\rho)n} d_n(l)[1-d_n(l)] . \tag{30}$$

Writing $l=\mu/\nu$ (rational) and $n=\alpha\nu+\beta$ with $\alpha=0,1,2,\ldots,\infty$ and $\beta=1,2,\ldots,\nu-1$ we get the finite sum

$$S\left[l=\frac{\mu}{\nu}\right] = \frac{-1}{1-e^{-\nu\gamma_0(\rho)}} \sum_{\beta=1}^{\nu-1} e^{-\gamma_0(\rho)\beta} d_\beta\left[\frac{\mu}{\nu}\right] \times\left[1-d_\beta\left[\frac{\mu}{\nu}\right]\right] . \tag{31}$$

For two classes of rational numbers μ/ν we can immediately perform the above β summation (apart from the trivial case $\nu=1$, with vanishing S). If

$$l\in C_a:\left[l=\frac{1}{Q};Q=1,2,3,\ldots\right] \tag{32}$$

we have

$$d_\beta\left[\frac{1}{Q}\right] = \frac{\beta}{Q} \quad \text{for } \beta<Q \tag{33}$$

if

$$l=l\in C_d:\left[l=\frac{Q}{Q+1};Q=1,2,3,\ldots\right] \tag{34}$$

we get, after trivial transformations,

$$d_\beta\left[\frac{Q}{Q+1}\right] = 1-\frac{\beta}{Q+1} \quad \text{for } \beta\leq Q . \tag{35}$$

Thus for both classes S is reduced to two geometric series. Only one further consideration is required if

$$l=l\in C_b:\left[l=\frac{2}{2Q+1};Q=1,2,3,\ldots\right] . \tag{36}$$

In this case we have to split the β sum into two because

$$d_\beta\left[\frac{2}{2Q+1}\right] = \begin{cases} \dfrac{2\beta}{2Q+1} & \text{for } \beta=1,\ldots,Q \\ \dfrac{2\beta}{2Q+1}-1 & \text{for } \beta=Q+1,\ldots,2Q . \end{cases} \tag{37}$$

It is straightforward to investigate the sum $S(l)$ in closed form for larger values of the enumerator μ. [The enumerator determines the functional form of $S(l)$, $l=\mu/\nu$.] But, for the purposes of this work the results for the above classes are sufficient. Abbreviating

$$A(\rho)=\frac{\pi^2\rho^2}{(\rho+\rho^2/4)^{1/2}}\frac{e^{-\gamma_0(\rho)}}{(e^{-\gamma_0(\rho)}-1)^2} \tag{38}$$

we finally obtain for the basic free energy

$$F_l^0(\rho,\Delta)+2\pi l\Delta=A(\rho)\begin{cases}\dfrac{1}{Q}\coth\left[\dfrac{\gamma_0(\rho)Q}{2}\right], & l\in C_a\\ \left[(Q-1)\coth\left[\dfrac{\gamma_0(\rho)}{2}\right]+\coth\left[\dfrac{\gamma_0(\rho)}{2}(Q+1)\right]\right]\dfrac{1}{Q+1}, & l\in C_d\\ \dfrac{2}{2Q+1}\dfrac{(1+e^{-\gamma_0(\rho)Q})(1+e^{-\gamma_0(\rho)(Q+1)})}{1-e^{-(2Q+1)\gamma_0(\rho)}}, & l\in C_b\ .\end{cases} \tag{39}$$

These are the first exact results for the free energy of the discrete parabola FK model and by (15) and (19) we get exact free energies for the coupled system with vanishing and infinite stiffness, respectively.

IV. DISCUSSION OF THE EXACT RESULTS; PHASE DIAGRAMS

In this section we will discuss the results for the free energies (11), (15), and (19) using winding numbers of the classes given in Eqs. (32)–(39). Before we discuss the possibility of phase transitions occurring we have to clarify the notation of "second-order" transition in this context. We have already introduced the winding number l as an order parameter. The problem here now is that the free energy does not depend analytically upon l. For a first-order transition this causes no problems, since the transition occurs discontinuously between two distinct values of l. We then *define* the transition to be of second order from a state $l=0$ to a state $l\neq 0$ if the following three conditions are fulfilled:

(a) $l=r_0/s_0$ and is rational,

(b) the free energy $F(l)$ is a convex function of l, and

(c) the limit $\lim_{s_0\to\infty}[F(l)-F(0)]/l=0$ exists for a certain "critical" combination of parameters controlling $F(l)$. (This is of course a sufficient condition, l does not necessarily have to be rational.)

In Fig. 3 we show $F^0(l)$ for $l\in C_a, C_b$ [Eq. (39)] at different misfit values Δ and constant $\rho=1.0$. For the coupled system with soft strain ($u=0, v\neq 0$), Fig. 3 gives on a different absolute scale the free energy for the rescaled values of $\rho=1-v^2$, and $\Delta=1.3(1-v^2)$, etc. We see that above a critical value for the misfit the winding number $l=0$ corresponds no longer to the minimum free energy, but l takes on all rational numbers in growing succession. The convexity condition (b) for $F^0(l)$, proved by Aubry, ensures the absence of a lower minimum at larger values of l. The limit condition (c) then defines the transition point and ensures a "practically" continuous transition from zero to nonzero values of l.

From the results for the class C_a [39] winding numbers we determine the critical misfit parameter $\Delta^{(0)}(\rho)$ at the transition point

$$\Delta^0(\rho)=\frac{1}{2\pi}A(\rho)\ . \tag{40}$$

This is plotted in Fig. 4. As just mentioned, these results may immediately be mapped onto the case ($u=0, v\neq 0$). In the limit $\rho\to 0$ Eq. (40) simplifies to $\Delta^0(\rho)=(\pi/2)\sqrt{\rho}$ in accordance with the corresponding result for the continuum model.

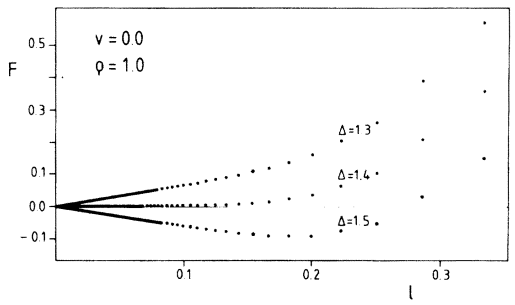

FIG. 3. Frenkel-Kontorova free energy $F^0(\rho,\Delta)$ as a function of the winding number $l\in C_{a,b}$ at constant potential strength ρ and different misfit values Δ. At small winding numbers the very dense dots are replaced by continuous lines.

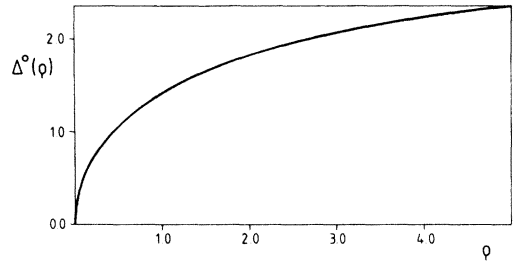

FIG. 4. Critical misfit $\Delta^0(\rho)$ for the second-order transition of the FK model.

Based on (39) Fig. 5 shows a phase diagram for the FK case $v=0$ (or, with obvious modifications for the eFK case with stiffness, $u=0$). Three remarks should be made at this point.

(i) In the noncommensurate regime ($l\neq 0$), $\Delta > \Delta^0(\rho)$, regions with specific rational values of l are separated by borderlines. But we have only shown a few classes of rational winding numbers (39). The inclusion of more classes expands the borderlines into narrow regions of widths (in Δ direction) decreasing exponentially with increasing denominator of the winding number. Hence, each winding number is associated with a nonzero range of Δ values. This is the devil's staircase.

(ii) In the ρ-Δ regime of Fig. 5 the misfit ranges with $l \in C_b$ become smaller and smaller with growing potential strength ρ. Hence, in a numerical ground-state evaluation based on (39) they do not appear at higher ρ values if the Δ scale is not fine enough or if the computer works with too low a precision.

(iii) For misfit values slightly above criticality the misfit-value range, where a given (small) winding number is stable, is extremely small. Thus any numerical evaluation will give a finite jump of the winding number.

For a demonstration of points ii and iii Table I gives some misfit values, at which the winding number changes, and the corresponding free energy.

To get an impression of the Δ scale, on which the small winding numbers l of the devil's staircase are taken, we use (39) for class C_a and $l \to 0$. Then

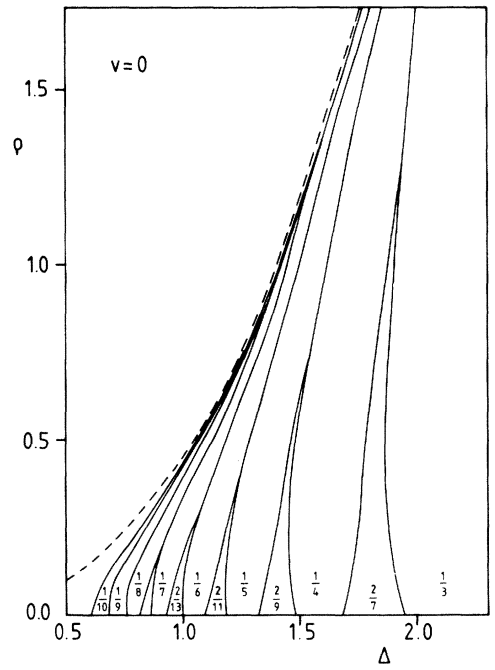

FIG. 5. Phase diagram for the FK system. Dashed line is the critical line from Eq. (40).

$$\Delta(l) \approx \Delta^0(\rho)\left[1+\frac{2}{l}\gamma_0(\rho)e^{-\gamma_0(\rho)/l}\right] \tag{41}$$

gives for $l \to 0$ the order of magnitude of that misfit, where l becomes stable.

We now turn to the case of an infinitely stiff, coupled system: $u=\infty, v\neq 0$. As Fig. 6 shows, the additional term $-\frac{1}{2}(2\pi v l)^2$ in the free energy (19) changes the nature of the phase transition: There is a finite jump of the winding number at the transition, it is thus of first order. Hence, we see that although the uncoupled and the completely stiff coupled systems are both represented by the same ψ,ϕ map, they do not even allow any conclusions about the type of transition. Figure 7 shows for different couplings v the critical misfit $\Delta^v_{u=\infty}(\rho)$, at which the transition takes place, and for some ρ values the corresponding jump of the winding number. To complete this section we give in Fig. 8 a phase diagram for $u=\infty, v=0.25$.

V. GENERAL RESULTS FOR ARBITRARY STIFFNESS u AND COUPLING v

With respect to the u-v plane of parameter space we have been able to give exact results on the boundary lines. The questions we want to answer in the following are to what extent is it possible to penetrate into the inner region of the u-v plane and how the tricritical line $v=1-\sqrt{u}$ known from the continuum approximation[4] appears.

We first introduce Fourier transforms such as

TABLE I. Visible part of the devil's staircase for $\rho=1.0$, $v=0.0$ if $l\in C_{a,b}$ and at a misfit-value resolution of 10^{-12}. W gives the stair width.

Δ	l	$10^{12}W$	$F_l^0(\rho=1.0,\Delta)$
1.404 962 946 208	0		0
1.404 962 946 209	$\frac{1}{34}$	1	−0.000 000 000 000 15
1.404 962 946 210	$\frac{1}{33}$	1	−0.000 000 000 000 34
1.404 962 946 211	$\frac{1}{32}$	4	−0.000 000 000 000 54
.			
.			
.			
1.404 962 946 215	$\frac{1}{31}$	9	−0.000 000 000 001 33
.			
.			
.			
1.404 962 946 224	$\frac{2}{61}$	1	−0.000 000 000 003 15
1.404 962 946 225	$\frac{1}{30}$	24	−0.000 000 000 003 36
.			
.			
.			
1.404 962 946 249	$\frac{1}{29}$	61	−0.000 000 000 008 39
.			
.			
.			
1.404 962 946 310	$\frac{2}{57}$	1	−0.000 000 000 021 61
1.404 962 946 311	$\frac{1}{28}$	155	−0.000 000 000 021 83
.			
.			
.			
1.404 962 946 466	$\frac{1}{27}$	394	−0.000 000 000 056 62

$$\psi_q=\frac{1}{\sqrt{N}}\sum_n e^{-iqn}\psi_n\ . \tag{42}$$

This transforms (5) into

$$F(u,v,\rho,\Delta)=F^0(\rho,\Delta)+\tfrac{1}{2}\sum_q\left|B_q\left[\frac{u}{\rho}\right]^{-1/2}\xi_q+vB_q\left[\frac{u}{\rho}\right]^{1/2}\psi_q\right|^2-\tfrac{1}{2}v^2\sum_q B_q\left[\frac{u}{\rho}\right]|\psi_q|^2 \tag{43}$$

with

$$B_q\left[\frac{u}{\rho}\right]=\frac{1}{1+\frac{2u}{\rho}(1-\cos q)}\ . \tag{44}$$

Equation (43) shows directly how ξ_q has to be chosen to minimize F:

$$\xi_q=-vB_q\left[\frac{u}{\rho}\right]\psi_q \tag{45}$$

(this means $\xi_n\sim-\sum_m e^{-\gamma_0(\rho/u)|m|}\psi_{n+1+m}$). What form does the free energy now take with (45)? In the position-space representation we get

$$F(u,v,\rho,\Delta)=F^0(\rho,\Delta)-\tfrac{1}{4}v^2\frac{\rho^2/u^2}{\left[\frac{\rho}{u}+\frac{\rho^2}{4u^2}\right]^{1/2}}\sum_{m=1}^{\infty}e^{-\gamma_0(\rho/u)m}\sum_n(\phi_{n+m}-\phi_n)^2 \tag{46}$$

(for $\rho/u\neq 0$; but the case $\rho/u=0$ we know already). A partly Fourier-transformed version reads

$$F_l(u,v,\rho,\Delta)=-2\pi l\Delta+\tfrac{1}{2}(1-v^2)(2\pi l)^2+\frac{\rho}{N}\sum_n V(\phi_n)+\frac{1}{2N}\sum_{q\neq 0}|\psi_q|^2\left[1-v^2B_q\left[\frac{u}{\rho}\right]\right]. \tag{47}$$

Equation (46) shows that due to the coupling to the strain, the FK model with its nearest-neighbor interaction is replaced by a system with harmonic interactions between all lattice sites. The exponential decrease of the coupling strength with distance is determined by the Lyapunov exponent $\gamma_0(\rho/u)$ defined in (12). Equation (47) demonstrates the instability of the system for $v^2\geq 1$: Taking $\phi_n=nl2\pi$ and $l=\text{integer}=\tau$ yields $F=-2\pi\tau\Delta+\frac{1}{2}(1-v^2)(2\pi\tau)^2$, i.e., $F\to-\infty$ if $\tau\to\infty$, the system explodes. Moreover, (47) can be used to find the ground state in the limit of vanishing potential. For a given winding number l this is given by $\psi_n=2\pi l$. The absolute ground state requires $l=\Delta/2\pi(1-v^2)$.

So far we have not used the condition $\partial F/\partial\phi_n=0$. Considering the parabola system again, this condition connects the phases and the parabola numbers via

$$\phi_q\omega_q^2=2\pi\rho m_q\ . \tag{48}$$

Here

$$\omega_q^2=\rho+2(1-\cos q)-v^2\frac{2(1-\cos q)}{1+\frac{2u}{\rho}(1-\cos q)} \tag{49}$$

gives the frequencies of small oscillations around the commensurate state. Obviously, $\omega_q^2\geq\rho$ in the stable coupling range $v^2<1$. Equation (48) is not correct for configurations with any particle on a potential cusp. However, reasoning analogously to the proof following Eq. (22), these are excluded from the set of ground-state configurations. With (48) the free energy looks quite simple:

$$F_l(u,v,\rho,\Delta)=-2\Delta\pi l+2\pi^2\rho\sum_q^{(l)}|m_q|^2\left[1-\frac{\rho}{\omega_q^2}\right]. \tag{50}$$

The vanishing of $1-\rho/\omega_q^2$ at $q=0$ guarantees the m_0 independence of F for $m_n=m_0$, thus expressing the translational invariance with respect to m. In the cases essentially transformable onto the FK model we obtained a free energy (23) with exponentially decreasing harmonic m interactions. All other cases, however, are more complicated. Now there are two contributions to the m interactions with different (and not in any case real) exponents. Abbreviating

$$K_\pm(u,v)=\frac{1}{2u}\{1+u-v^2\pm[(1+u-v^2)^2-4u]^{1/2}\}\ , \tag{51}$$

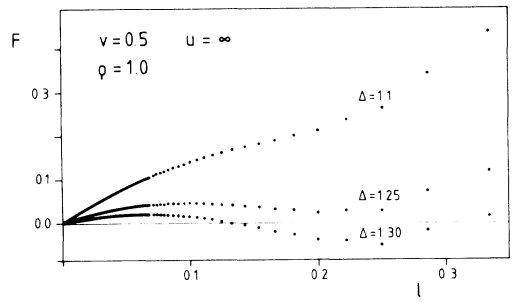

FIG. 6. Free energy as a function of the winding number $l\in C_{a,b}$ in the limit of infinitely stiff ($u=\infty$) substrate. As in Fig. 3 the dots at small l values are replaced by continuous lines.

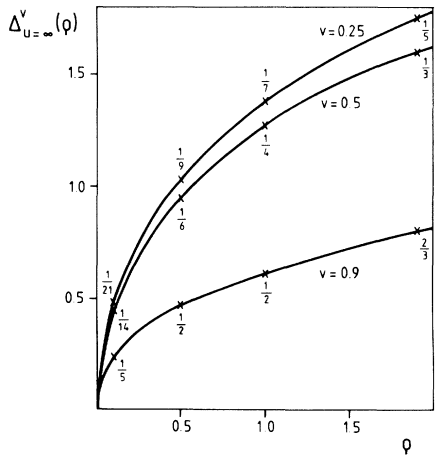

FIG. 7. Critical misfit $\Delta^v_{u=\infty}(\rho)$ of the system with infinitely stiff ($u=\infty$) substrate at different couplings v. For some ρ values the jump of the winding number of the first-order transition is indicated.

$$\cosh\nu_\pm = 1+\frac{\rho}{2}K_\pm, \quad \mathrm{Re}\nu_\pm > 0$$

we get for $K_+ \neq K_-$

$$F_l(u,v,\rho,\Delta)+2\pi l\Delta = \sum_{n=1}^{\infty}[e^{-\nu_+ n}f_+(K_\pm,\nu_+,u,\rho) + e^{-\nu_- n}f_-(K_\pm,\nu_-,u,\rho)]\Omega_n^{(2)}(l) \quad (52)$$

with $\Omega_n^{(2)}(l)$ given in (24), and for $K_+ = K_- (\nu_+ = \nu_- = \nu)$

$$F_l(u,v,\rho,\Delta)+2\pi l\Delta = \sum_{n=1}^{\infty} e^{-\nu n}[f_1(\rho,u)+f_2(\rho,u)(1-\sqrt{u}\,)n]\times\Omega_n^{(2)}(l)\,. \quad (53)$$

The f functions are defined as follows:

$$f_\pm = \pm\pi^2\rho\frac{1-\dfrac{1}{uK_\pm}}{K_+-K_-}\frac{\cosh\nu_\pm-1}{\sinh\nu_\pm},$$

$$f_1 = \frac{\pi^2\rho^2}{\sinh\nu}\frac{1+\dfrac{1}{\sqrt{u}}+\dfrac{\rho}{2u}}{2+\rho/2\sqrt{u}}, \quad (54)$$

$$f_2 = \frac{\pi^2\rho^2}{\sinh\nu}\frac{\left[\dfrac{\rho}{2\sqrt{u}}\right]^{1/2}}{\sqrt{2}+\dfrac{\rho}{2\sqrt{u}}}.$$

Before exploiting this form (51), we will quickly discuss analogies to the continuum model. The ρ-independent quantities $K_\pm$ are just those eigenvalues of the same name appearing in the continuous theory[4] $\rho\to 0$, and $K_+ = K_-$ defines those curves S_{I} ($v = 1-\sqrt{u}$) and S_{II} ($v = \sqrt{u}-1$) that have already separated in the continuous case the u-v plane into three regions (Fig. 9). Brocksch *et al.*[4] demonstrated that in region I the transition is of second order and that in regions II and III it is of first order (S_{I} thus being a tricritical line). Region III differed from II by an oscillatory behavior of the free energy. Concerning (52) we can see a positive harmonic interaction between m_i and m_{i+n} for all distances n if we are in region I or on the line S_{I}. In region II and on S_{II} the interaction is positive for small distances and negative at large n values. Finally, in region III the exponents $\nu_\pm$ are complex and the interaction shows alternating sign, being positive for small distance n. The always positive interaction in region I represents essentially the same behavior as the FK model [Eq. (23)], thus a second-order transition in I

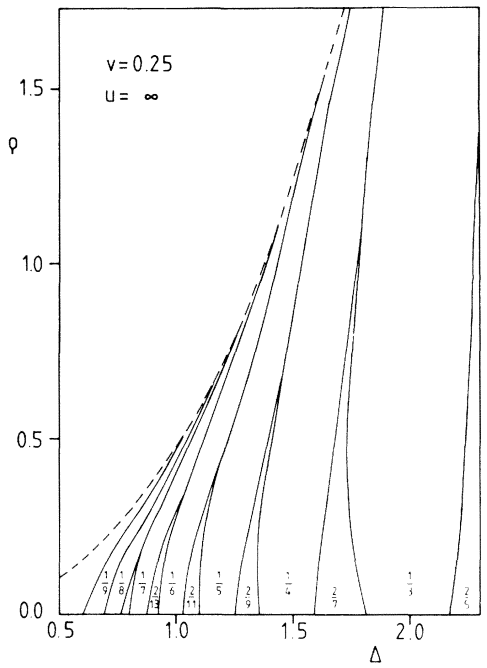

FIG. 8. Phase diagram for coupling $v=0.25$ and infinitely stiff substrate. All boundary lines end at different points of the (dashed) critical line.

is very obvious.

It remains now to investigate the second moment (24) in more detail. If we write the integer numbers m_{i+n}-m_i as

$$m_{i+n}-m_i = \mathrm{Int}(nl)+d\,, \quad d = 0,\pm1,\pm2,\ldots \quad (55)$$

and if we associate with each d a probability $P_d^{(n)}$ characterizing how often m_{i+n}-m_i obeys (55) with a fixed d in the sum (24), we can express the second moments by these probabilities. Taking into account the normalization $\sum_d P_d^{(n)} = 1$ and fixing the

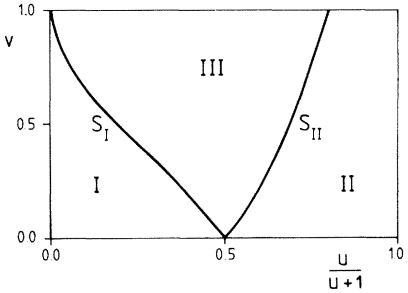

FIG. 9. Separating lines $S_{\mathrm{I}}, S_{\mathrm{II}}$ of the u-v parameter plane.

first moment [Eq. (25)] we obtain

$$\Omega_n^{(2)}(l) = -\mathrm{Int}(nl)^2 - \mathrm{Int}(nl) + nl[1+2\,\mathrm{Int}(nl)] + \sum_{d\neq 0,1} P_d^{(n)} d(d-1) \; . \tag{56}$$

As $\sum_{d\neq 0,1} P_d^{(n)} d(d-1) \geq 0$, the second moment $\Omega_n^{(2)}(l)$ is minimized, if only the probabilities $P_0^{(n)}$ and $P_1^{(n)}$ are different from zero. This was just the case for m_n given by (26), which shows that the ground-state energy of the FK system can be found by minimizing the free energy in the form (23). This is not a trivial point, because the m variables cannot be chosen arbitrarily but are related to the phases via (21), thus (22) and (21) have to be satisfied simultaneously. If the same minimization principle could be applied to the coupled $v\neq 0$ case too, we immediately could give exact free energies in region I.

What we can prove at the moment by perturbation theory, however, is that the m_q and thus the second moment $\Omega_2^{(n)}(l)$ are just those of the FK case if we have $v^2\to 0$, or $u\to\infty$, or $u\to 0$. That is, the second moments as given by (27) are exact even in the vicinity of the boundary lines discussed in Sec. III A. The proof uses relations (21) and (48) and is demonstrated here for small perturbations $v^2=\epsilon\to 0$. As was shown, there is no ground state $\{\phi_n^0\}$ of the systems of Sec. III A with any particle just on a cusp of the parabola potential. Thus we have

$$m_n^0 = \mathrm{Int}\left[\frac{\phi_n^0}{2\pi}+\frac{1}{2}\right] < \frac{\phi_n^0}{2\pi}+\frac{1}{2} < m_n^0+1 \; , \tag{57}$$

the inequalities holding in the strict sense. If, by including the perturbation ϵ, ϕ_n changes continuously, $\phi_n/2\pi+\frac{1}{2}$ will remain in the open interval (m_n^0, m_n^0+1) for ϵ sufficiently small. But then

$$m_n = m_n^0 \quad \text{for} \quad \epsilon\to 0 \; . \tag{58}$$

It remains to show that this is in accordance with (48). If we define

$$R_q = \frac{2(1-\cos q)}{\left[1+\frac{2u}{\rho}(1-\cos q)\right]\left[1+\frac{2}{\rho}(1-\cos q)\right]} \; , \tag{59}$$

we can write (48) as

$$\phi_q \omega_q^2(\epsilon=0)(1-\epsilon R_q) = 2\pi\rho m_q \; . \tag{60}$$

Equations (58) and (60) then give

$$\phi_q = \phi_q^0 \frac{1}{1-\epsilon R_q} \; . \tag{61}$$

Hence, the change of the phases is as small as desired if $\epsilon\to 0$, there is no contradiction to our above assumption, and (58) is valid. This proves that not only on the boundary lines $v=0$, $u=0$, or $u=\infty$, but also to leading order in their vicinity, the ground states have $m_n=\mathrm{Int}(nl+\alpha)$ and second moments as given in (27). Comparing (23) with (52) and using (38) and (39) we can immediately write the free energies in these regions. Confining ourselves, e.g., to the winding numbers of class C_a [Eq. (32)] we have

$$F_{l=1/Q}(u,v,\rho,\Delta) = \frac{1}{Q}\left[-2\pi\Delta + f_+ \frac{e^{-\nu_+}}{(e^{-\nu_+}-1)^2}\coth\frac{\nu_+ Q}{2} + f_- \frac{e^{-\nu_-}}{(e^{-\nu_-}-1)^2}\coth\frac{\nu_- Q}{2}\right] \tag{62}$$

with $Q=1,2,\ldots$.

In Fig. 10 we show the application of (62) for $\rho=1.0$, $v=0.1$, and $u=1.22$. Hence, we have just entered region II of the u-v plane and are still rather close to the line S_{I}—the tricritical line from the continuous approximation. From the continuous approximation one therefore expects a first-order transition. Since (62) indicates a second-order transition for region I, and since we find for $\rho=1$, $v=0.1$, and $u=\infty$ (infinite stiffness of the substrate) a jump of the winding number from $l=0$ to $l=\frac{1}{9}$, we can expect a jump into a winding number $0<l\lesssim\frac{1}{9}$. In fact, (62) produces—as Fig. 10 shows—a jump into $l\approx\frac{1}{23}$. We want to point out that very high precision in the misfit value is required to detect the nature of the transition in this u-v region. Figure 10 shows free energies before and after the transition at misfits differing only in the tenth decimal place. With a precision of eight digits it is not possible to

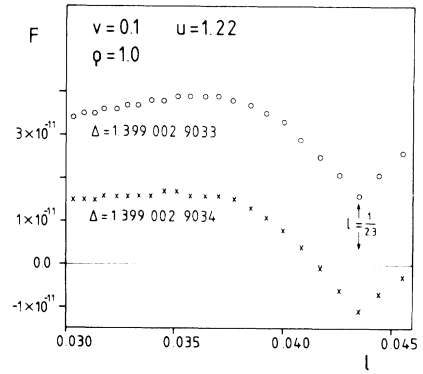

FIG. 10. Free energies at parameters $v=0.1, u=1.22$ (i.e., region II near S_{II}, see Fig. 9), and $\rho=1.0$ for misfits just above and below the first-order transition.

identify the nature of the transition. Obviously, energy differences of order 10^{-11} are important, compared to values of order 10^{-1} typical near the $u=\infty$ boundary. The critical misfit value $\Delta_{u=1.22}^{v=0.1}(\rho=1)\approx 1.3990$ is not significantly smaller than $\Delta_{u=\infty}^{v=0.1}(\rho=1)\approx 1.402$.

We can not make a definite prediction about the range of validity of the above perturbation analysis. In any case, it supports the quantitative feeling—also based on the continuum version for $l\to 0$—that the change of the phase transition from second to first order is caused by the appearance of an attractive potential in Eq. (52).

VI. CONCLUDING REMARKS

We have shown in this paper that the interpretation of variational equations for lattice structures as discrete maps is a useful, albeit not nearly sufficient, concept to understand the mechanism of phase transitions to superstructures. The use of computers for explicit brute force evaluation of free energies is severely hampered by the sensitivity of the results to small truncation errors. The most useful tool of general applicability was found to be the approximation of irrational numbers by rationals as a consequence of piecewise linearizations plus matching conditions, just as in elementary quantum mechanics. This is in some sense complementary to the procedures in discrete maps representing dynamic systems. There the recursion relations often do not require the additional selection of trajectories by absolutely minimizing a generating functional and thus allow one to employ the powerful concept of self-similarity and renormalization directly on the map.

The extension of these procedures to higher-dimensional systems is not easy. A layerwise mean-field approximation, leading to effectively one-dimensional models, however, has proven to be useful for the understanding of inhomogeneous solids. We therefore expect quite a number of interesting problems in the formation of compound materials to be tractable by these techniques.

---

[1](a) S. Aubry, in *Solitons and Condensed Matter Physics,* Springer Series in Solid-State Sciences 8, edited by A. R. Bishop and T. Schneider (Springer, New York, 1978); (b) S. Aubry in *Seminar on the Rieman Problem, Spectral Theory and Complete Integrability,* Springer Lecture Notes in Mathematics, edited by David S. Chudnovsky (Springer, New York, 1981); (c) S. Aubry, P. Y. LeDaeron, and G. André (unpublished).

[2](a) Y. I. Frenkel and T. Kontorova, Zh. Eksp. Teor. Fiz. 89, 1340 (1938); Phys. Z. Sowjetunion 13, 1 (1938); (b) F. C. Frank and J. H. van der Merwe, Proc. R. Soc. London, Ser. A 198, 205 (1949).

[3](a) B. Chirikov, Phys. Rep. 52, 265 (1979); (b) J. M. Greene, J. Math. Phys. 20, 1183 (1979); (c) Scott J. Shenker and L. P. Kadanoff, J. Stat. Phys. 27, 631 (1982).

[4]H. J. Brocksch, H. U. Everts, and H. Müller-Krumbhaar, J. Phys. C 14, 603 (1981). The model was originally proposed by P. Bak and J. Timonen, J. Phys. C 11, 4907 (1978), but incorrectly treated.

[5]A. D. Bruce, R. A. Cowley, and A. F. Murray, J. Phys. C 11, 3591 (1978).